Earth and Planetary Science Letters 400 (2014) 66–76

Contents lists available at ScienceDirect

Earth and Planetary Science Letters

www.elsevier.com/locate/epsl

The secondary crater population of Mars

Stuart J. Robbins [a,*], Brian M. Hynek [b]

[a] Laboratory for Atmospheric and Space Physics, University of Colorado at Boulder, 3665 Discovery Dr., Boulder, CO 80309, United States
[b] Laboratory for Atmospheric and Space Physics and Department of Geological Sciences, University of Colorado at Boulder, 3665 Discovery Dr., Boulder, CO 80309, United States

ARTICLE INFO

Article history:
Received 7 December 2013
Received in revised form 22 March 2014
Accepted 8 May 2014
Available online 5 June 2014
Editor: C. Sotin

Keywords:
Mars
craters
surface ages

ABSTRACT

Impact craters ("craters") are ubiquitous across most solid surfaces in the Solar System. The most common use of crater populations (populations as defined by diameter- or "size-" frequency) is to estimate relative and absolute model surface ages based on two assumptions: Craters will form spatially randomly across the planetary body, and craters will form following a random distribution around a known or assumed temporal flux. Secondary craters – craters that form from the ejecta of a crater formed by an extraplanetary-sourced impactor – belie both of these assumptions and so will affect crater-based ages if not removed from crater counts. A question unanswered with observational data to this point has been, what is the population of primary versus secondary craters on a given planet? We have answered this question for Mars for craters larger than 1 km in diameter by using a recently published global crater database, classifying craters as primary or secondary, and creating maps of the population statistics. Our approach was to err on the side of a crater being primary by default and hence our work is a conservative measurement. We show that, globally, secondary craters are at least 24% as numerous as primary craters (comprising 19% of the total population) for diameters $D \geq 1$ km. However, there are many "hot spots" across the globe where secondary craters are more numerous than primary craters for diameters as large as 9 km. This is the first time such a study has been conducted globally for any body and it shows that, not only are secondary craters numerous, but they can significantly affect crater populations in a non-uniform way across a planetary surface.

1. Introduction

Identification and measurement of craters on solid surfaces is the only way to estimate absolute ages on objects without returned samples, akin to the *Apollo* and *Luna* missions. This common practice has been refined and utilized for decades (*e.g.*, Shoemaker et al., 1970; Crater Analysis Techniques Working Group, 1979; Neukum, 1983; Neukum et al., 2001; Hartmann, 2005), but the basic idea remains the same: A surface is older than another if it has a greater crater density because it must have been accumulating craters for a longer period of time. Two fundamental assumptions of crater age-modeling is that crater formation is random across the planetary body and follows a known (or assumed) flux through time.

Over half a century ago, Shoemaker (1962) identified the issue of secondary craters on planets (craters that form from the ejecta of a larger primary impact event and are necessarily smaller). The subject of secondary craters was controversial for the next several decades (*e.g.*, Neukum and Ivanov, 1994), though observational studies were relatively few (*e.g.*, Guinness and Arvidson, 1977; Tanaka, 1986; Strom et al., 1992; Neukum and Ivanov, 1994), until the mid-2000s when Bierhaus et al. (2005) identified $>10^4$ secondary craters that contaminate crater statistics on Jupiter's moon Europa, and McEwen et al. (2005) identified $>10^6$ secondary craters around the pristine crater Zunil on Mars. Both of these studies focused on relatively small surface areas indicating large – if localized – secondary crater contribution to crater statistics. Now that there is general consensus that they exist and contaminate populations, it must also be recognized that the two assumptions of crater-based ages are false when secondary craters are concerned: They form in large numbers in a geologic instant and their locations are correlated with and centered upon the primary crater that sourced them.

Understanding the role secondary craters have on local and global crater statistics is important, if only to verify the null hypothesis that they do not significantly contaminate the population of craters larger than a given diameter, one that has had observational (*e.g.*, Neukum et al., 1975) and recent theoretical

* Corresponding author.
E-mail addresses: stuart.robbins@colorado.edu (S.J. Robbins), hynek@lasp.colorado.edu (B.M. Hynek).

http://dx.doi.org/10.1016/j.epsl.2014.05.005
0012-821X/

support (*e.g.*, Werner et al., 2009). Secondary fields are typically manifest as a visible and tight annulus around the primary, though recent work has shown that secondary fields can be several thousand kilometers from the primary (Shoemaker et al., 1994; Preblich et al., 2007; Robbins and Hynek, 2011a). With current and forthcoming high-resolution imagery of Mars, the Moon, Mercury, Vesta, Ceres, Pluto and Charon, and numerous Saturnian satellites, and impact crater studies focusing on ever smaller craters, a better understanding of secondary crater ("secondaries") populations and their contamination of primary crater ("primaries") statistics is more important than ever.

Traditionally, secondaries are divided into two categories. The first are adjacent secondaries that typically form a distinct high-spatial density annulus of small craters around the primary, and the second are distant secondaries that are often found in clusters within rays but which also contribute to the apparently random spatial distribution of small craters (so-called "background secondaries" that are still the most controversial in the literature). Work has been done towards better understanding these populations by other authors (*e.g.*, Bierhaus et al., 2005; McEwen et al., 2005; Preblich et al., 2007), and we have also investigated both "near-field" (Robbins and Hynek, 2011b) and "far-field" (Robbins and Hynek, 2011a) secondary craters. The work we present herein, however, ignores that classification and was, instead, a search to identify all secondaries on Mars that are present within a global Mars crater database that contains a statistically complete sample of all craters $D \geq 1$ km; we explain our technique for doing this identification in Section 2. In so doing, we have been able to put the first observational constraints on the global population of secondary craters on Mars and create local and regional maps of the contamination level and contamination diameter of the overall crater population by secondary craters (Section 3). We discuss implications for this not only to studies on Mars but also to other solar system objects in Section 4.

2. Methods

The Robbins and Hynek (2012) crater database contains approximately 640,000 Martian craters, approximately 385,000 of which form a generally complete census of all craters $D \geq 1$ km. Craters were visually identified in GIS software using 100 m/pix global THEMIS (THermal EMission Imaging System) Daytime IR mosaics (Edwards et al., 2011), and rims were mapped using *ArcMap*'s edit tools. Additional searches for craters were made using MOLA gridded data at 1/128° scale (Smith et al., 2001). Polygons representing crater rims were fit with a non-linear least-squares (NLLS) circle-fit algorithm to calculate each crater's diameter and center latitude and longitude after correcting for map projections. It is important to note that craters were identified regardless of morphology for this database, hence it is representative of all craters $D \geq 1$ km, both primary and secondary, on Mars. Due to the data source, this analysis is therefore limited to craters $D \geq 1$ km. The remainder of this section describes only how the database was analyzed and results displayed (Figs. 2–5), leaving interpretation in Section 3.

2.1. Secondary crater identification technique

For this work, the global THEMIS mosaic of Mars was searched twice for secondary craters – first to identify them, second to search for missed secondaries and accidentally included primaries. Once completed, all craters identified as secondaries were mapped on the same global mosaic and examined individually for false positives (primary craters identified as secondaries).

The distinction between primary and secondary craters themselves is, unfortunately, not as objective as one may hope. The distinction was made based on crater morphology and classic morphologic characteristics of secondary craters (Shoemaker 1962, 1965; Oberbeck and Morrison, 1974; McEwen and Bierhaus, 2006; Robbins and Hynek 2011a, 2011b): (1) Is the crater entrained within a chain, elongate crater group, and/or has a "herringbone" ejecta pattern? (2) Is the crater highly elliptical with the long axis radial to a much larger crater? (3) Does the crater appear to have been "scooped" out at an angle with the shallower part radially away from a larger crater? If a crater fit some of these, it was marked as a probable secondary crater; numerous examples of these are found in Fig. 1 along with primaries to show the differences. If the crater did not fit any of these criteria, it was assumed to be a primary crater. In making this distinction, the bias was to err on the conservative side, only identifying the feature as a secondary crater if it was more likely than not, based on those criteria, to be a secondary crater. This method has the side-effect of including likely airburst features where a single impactor will breakup in the atmosphere and produce numerous, tightly clustered craters (Popova et al., 2007). However, while this is a contaminant, these kinds of crater clusters are themselves an additional contaminator of the primary crater population because, like secondaries, they form in a geologic instant and are tightly clustered spatially. Ergo, their removal – or an estimate of what crater would have formed from an intact impactor – would also be necessary for applications of primary craters such as age-modeling. Due to the method, this work will not identify the lone background secondaries that are indistinguishable from primaries, though we can still learn significantly from what is identifiable.

Once this process was complete, the secondary and primary crater populations could be analyzed and displayed. A scatterplot showing their global distribution is Fig. 2.

2.2. Determining the transition diameter globally and locally

The simplest way to estimate contamination by secondary craters is to determine at what diameter and location, if any, secondary craters dominate over the population of primary craters. To do this, one can create a standard size-frequency distribution (SFD) of each population (Fig. 3) (Crater Analysis Techniques Working Group, 1979). This can be done as a normal histogram to create an incremental SFD (ISFD) or as a cumulative version (CSFD) that is summed from large to small crater diameters. Both are shown in Fig. 3 and interpreted in Section 3 along with an R-plot version. This can be done globally, and it can be done for a given latitude/longitude range. The latter was constructed for Figs. 4 and 5.

The key idea behind a "transition diameter", D_t, is that on a SFD, primary craters have a shallower slope relative to secondary craters. Primaries typically have a slope of -3 on an ISFD and -2 on a CSFD (Neukum et al., 2001), while secondaries are steeper (McEwen and Bierhaus, 2006), ranging from about -3 to -8 on a CSFD and averaging approximately -5 (Robbins and Hynek, 2011a). Ergo, as secondary craters are produced, they will at some diameter become more numerous than primaries and the diameter at which they do is the transition diameter. The interpretation of D_t on an ISFD is where the *production* of secondaries and primaries are equal, for $D < D_t$ secondaries are produced more at a given diameter, and for $D > D_t$ primaries are produced more. The interpretation of D_t on a CSFD is where the *population* of craters $>D_t$ is comprised of primaries and $<D_t$ is comprised of secondaries.

To examine D_t across Mars, we used a moving average that could be created for a latitude/longitude grid of arbitrary resolution. This was done for $1° \times 1°$ binning in Figs. 4–5 for radii R around each bin center of 500 km, 1000 km, and 1500 km.

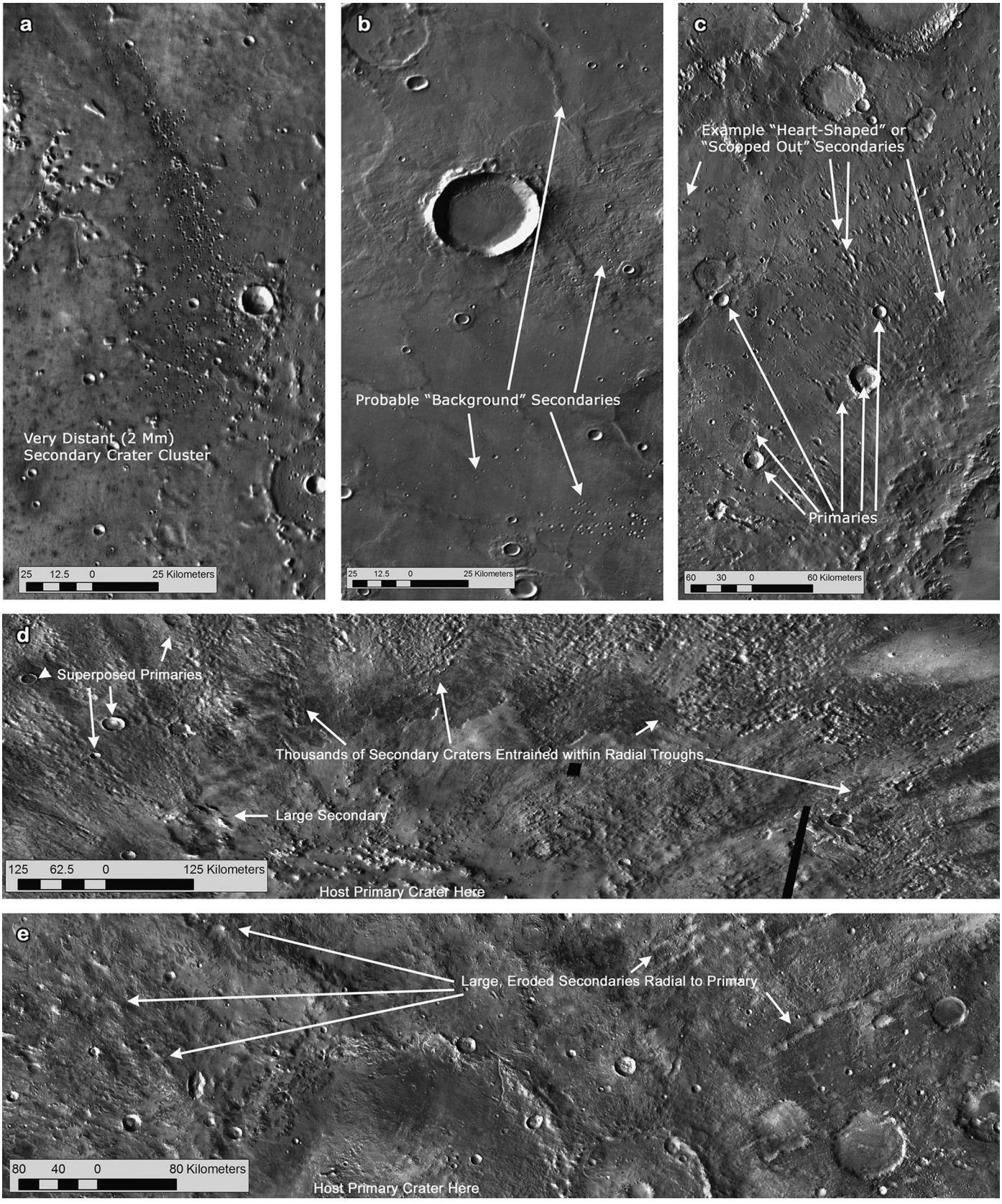

Fig. 1. Numerous examples of secondary craters, each panel highlighting different morphologies: (a) shows a cluster of secondary craters likely ejected from a crater ~2000 km distant (Robbins and Hynek, 2011a), (b) "background" secondary craters that are not necessarily in clusters but show other characteristics typical of secondary craters, (c) highly elongated craters with overlapping cavities and ejecta, (d) an extreme case of secondary craters in trough-like formation from a large primary, and (e) other trough-like entrainment. In (c) and (d), example primary craters have also been indicated.

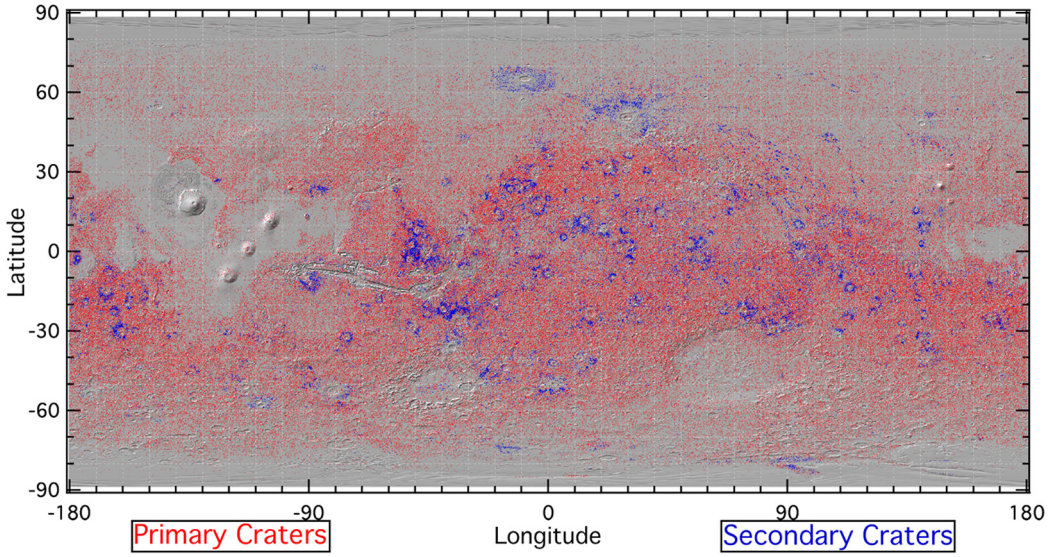

Fig. 2. Global population of $D \geq 1$ km craters, coded for primary and secondary craters by color (electronic) or shade (print). Data are overlaid on MOLA shaded relief (Smith et al., 2001).

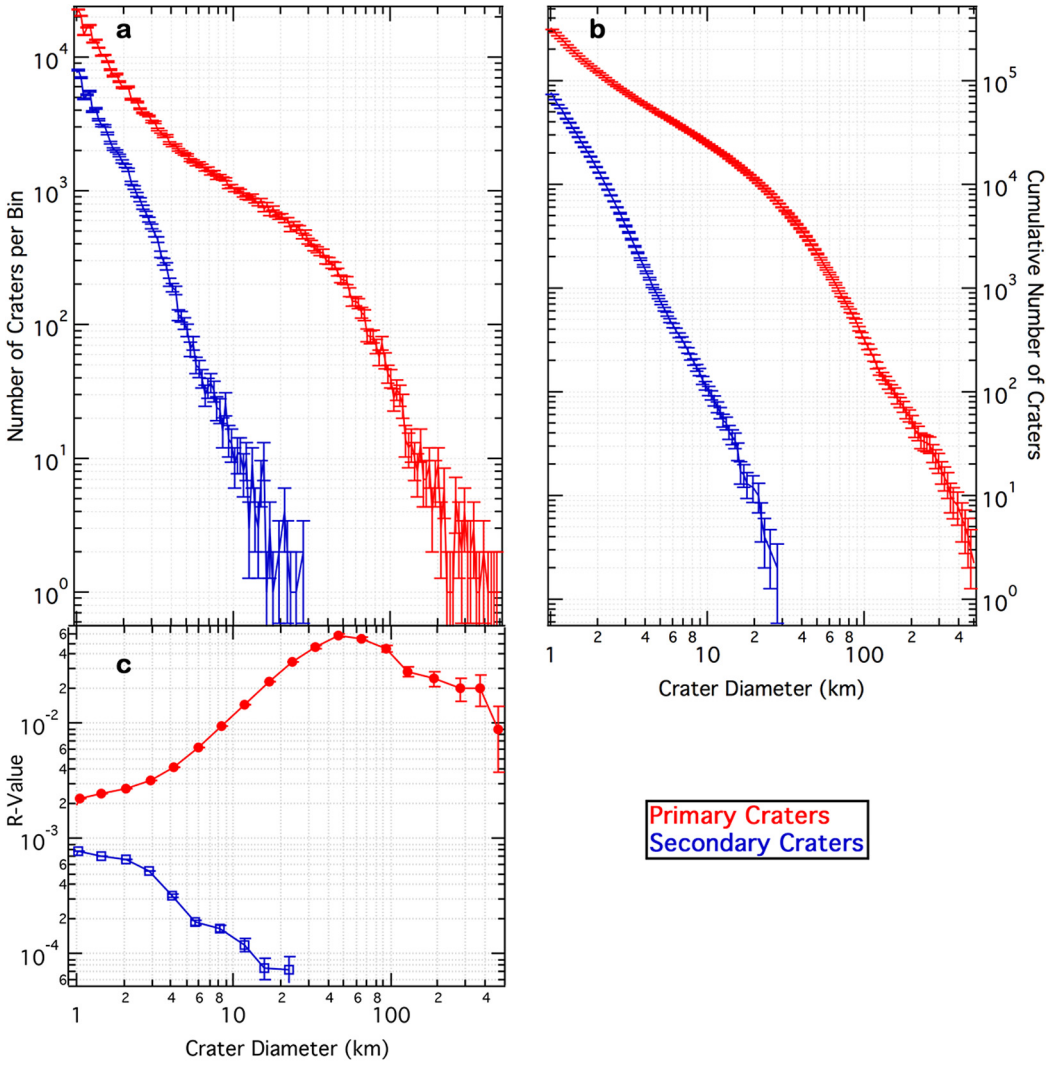

Fig. 3. Size-frequency diagrams (SFDs) for the global Mars results; legend is the same for both panels. Panel (a) shows incremental SFDs (ISFDs) while panel (b) shows cumulative results (CSFDs), and panel (c) shows an R-plot (Crater Analysis Techniques Working Group, 1979). The slight shallowing in the secondary crater SFDs for $D \lesssim 2$ km is likely due to under-identifying the secondary crater population at these diameters.

Within each area surrounding the center of each bin, CSFDs (Fig. 4) and ISFDs (Fig. 5) were constructed and if the secondary crater population reached a set fraction of the primary crater population, that diameter was saved as the bin value. In this manner, we created both local ($R = 500$ km) and regional ($R = 1500$ km) maps with high resolution ($1° \times 1°$) that show where secondary craters may comprise 50% the total population of craters (top row), 33% (middle row), and 25% (bottom row). Smaller radii could not be used due to the decreasing number of craters.

3. Global and local secondary crater populations and transition diameters

3.1. Global analysis

Historically, several researchers have avoided using $D < 5$ km Martian impact craters in part to avoid secondary crater contamination (*e.g.*, Tanaka, 1986; Barlow, 1988). Various observations and models have estimated at what diameter secondary craters may equal the primary crater population of Mars, as a global average (*e.g.*, Tanaka, 1986; Strom et al., 1992; Bottke et al., 2005; summarized in McEwen and Bierhaus, 2006). They estimate a transition diameter $D_t \approx 1$ km, where smaller diameter crater populations would be dominated by secondaries and larger craters by primaries. Using Fig. 3, the estimate based on SFDs can be tested.

For this analysis, it is more appropriate to use the CSFD version (Fig. 3b) because most researchers use all craters larger than a given diameter for crater population studies. From the database and Fig. 3b, there were 700 craters identified as secondaries $D \geq 5$ km, and there were 46,791 $D \geq 5$ km that remained primaries. This means secondaries are 1.50% as numerous as primaries for $D \geq 5$ km globally, or, they comprise 1.47% the total population of $D \geq 5$ km craters on Mars. This would suggest that one has a 1 in ~70 chance of a given crater $D \geq 5$ km being a secondary at any random location on the planet. This is typically well within the inherent factor of 2× uncertainty in crater chronology functions (Neukum et al., 2001) and factor of 15–45% uncertainty in whether features are even craters (Robbins et al., 2014).

One can then examine the estimate that $D_t \approx 1$ km on Mars. In this work, 72,208 craters $D \geq 1$ km were identified as secondary craters, while 308,998 remained primaries, meaning the total population of identifiable secondaries is 23% that of primaries, or, alternatively, they comprise 19% of the global population of craters $D \geq 1$ km. The ISFD (Fig. 3a) shows secondaries are produced at $\sim 20 \pm 3\%$ the frequency of primaries for the diameters near 1 km, or that they comprise $\sim 16 \pm 2\%$ of the total number of craters produced at that diameter.

As discussed in Section 2.1, it is likely that secondary craters were missed in this work, meaning their population was underestimated. At large, ~10–20 km diameters, one might expect to observe in Fig. 2 that large numbers of secondary craters would be seen surrounding very large $\gtrsim$1000 km craters such as Hellas and Argyre, as one sees around Orientale on the moon. However, this is not observed, nor is an over-density of these sizes of primary craters around these "basins", and there is no apparent uptick in the number of secondaries or primaries of these diameters in Fig. 3. Two possible *post hoc* reasons for this absence are: (1) Secondaries at these diameters have been removed by the large amounts of resurfacing between the Noachian and Hesperian (*e.g.*, Chapman and Jones, 1977; Tanaka et al., 1988; Craddock and Maxwell, 1993; Boyce and Garbeil, 2007), after these basins formed (*e.g.*, Werner, 2008; Fassett and Head, 2011; Robbins et al., 2013); (2) secondaries at these diameters have been so degraded by subsequent processes that they are indistinguishable, based on our methods, from large primaries. Unfortunately, both of these scenarios would seem to be untestable at this time, and it is likely that both have affected the secondary crater populations.

A failure to detect secondaries at small diameters is supported by examining the slope of the CSFD (and ISFD) in Fig. 3: The slope of secondary craters is roughly constant (−3.2) for $2.5 \lesssim D \lesssim 25$ km craters (except for a minor deficit near $D \sim 5$ km), but it is significantly shallower (−2.3) for $D \lesssim 2$ km (these were measured on the log (ISFD) per Chapman and Haefner, 1967). There is no theoretical reason why the slope of secondary craters should decrease at this large of a diameter, and many researchers including Robbins and Hynek (2011a, 2011b) have found it constant through $D = 1$ km over a large diameter range. Therefore, this is more likely an indication of failure to recognize secondary crater morphology for $D \lesssim 2$ km. If the −3.2 slope is extrapolated from $D = 2.5$ km through $D = 1$ km, the number of secondary craters would be $\approx$ 129,000, meaning primary craters would number $\approx$ 259,000. Then, secondary craters would be 50% as numerous as primaries and represent 33% of the total population of craters $D \geq 1$ km. This still indicates that $D_t \neq 1$ km unless this work under-estimated secondary craters by another factor of ~2× on top of the extrapolation of missed craters $D \lesssim 2$ km. Based on the extrapolation from $D \gtrsim 2$ km primary and secondary craters, it is estimated that $D_t \approx 0.78$ km (while this value is to two significant figures, it should be thought of as $\approx 3/4$ km rather than a two-significant-figure value). This result is close to $D_t \approx 0.6$ km, estimated by McEwen et al. (2005) for Hesperian-aged terrain which comprise much of the terrain where we classified secondary craters (see Section 3.3). Despite these findings, the fact that secondaries were measured to comprise ~20% the overall population of craters $D \geq 1$ km is not insignificant and, if one were in a linear region of the crater chronology curve ($\lesssim$3.5 Ga; Ivanov, 2001; Robbins, 2013, submitted for publication), then any ages using $D \geq 1$ km craters would be over-estimated by at least ~20% if secondary craters were not removed.

3.2. Local and regional analysis

While the global result gives an overview for the planet, more useful information can be gained by performing the same kind of analysis ("is there a diameter at which secondary craters dominate over primary?") for individual locations on the planet. After all, Fig. 2 clearly shows that the distribution of secondary craters is not uniform. Figs. 4–5 show this regional analysis: At what diameters secondary craters dominate over primary craters, for a given threshold (row), over a given area (column). CSFDs were used for Fig. 4 because they answer the question, "how small a crater diameter can be used before the number of secondary craters surpasses the number of primary craters?" ISFDs were used for Fig. 5 to answer the question, "at what crater diameter is the production and preservation of secondary craters equal to or greater than that of primary craters?"

At a broad, regional level (right column, Figs. 4–5), there is no area of the planet where secondaries are as numerous as primaries for $D \geq 1$ km; however, the area around Lyot crater (50°N, 30°E, $D \approx 220$ km; also shown as Fig. 1d) and eastward towards Lomonosov crater (65°N, −10°E, $D \approx 130$ km), is an area where there are as many secondaries as primaries for $D \lesssim 3.4$ km (Fig. 5, upper-left). This is expected because both Lyot and Lomonosov craters are relatively young features (Werner, 2008; Robbins et al., 2013), they are on relatively young and uncratered terrain, and, as large craters, they would be expected to form many secondary craters.

At a more local level, when the radius of interest is 500 km (left column, Figs. 4–5), the population of secondary craters produced (Fig. 5) equals that of primary craters $D \geq 1$ km in numerous lo-

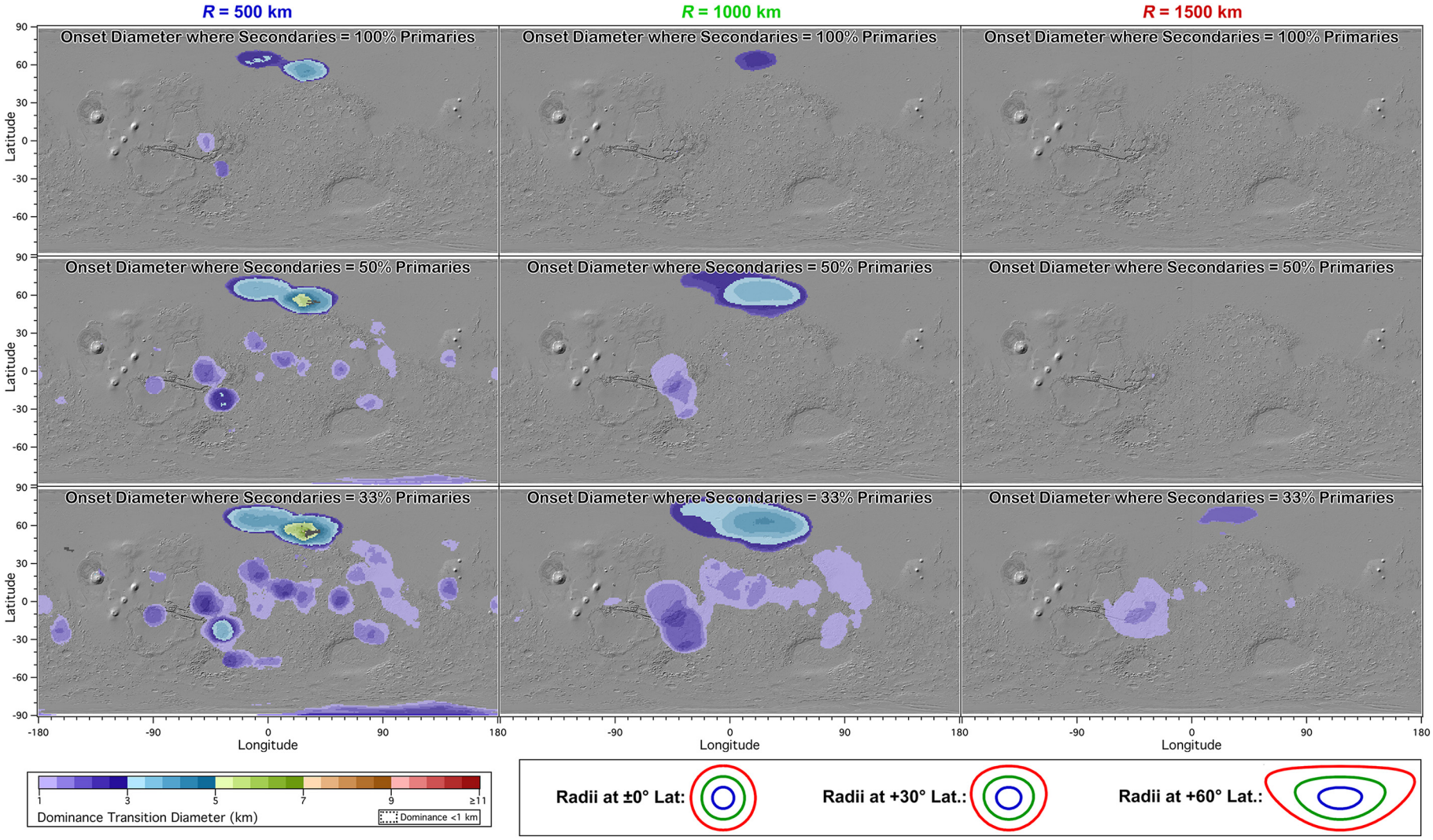

Fig. 4. The planet was binned in 1° latitude by 1° longitude. All craters within a radius of 500 km (left), 1000 km (center), and 1500 km (right) from the center of each bin were extracted from the final database (the size of each circle of interest is shown in the legend at the bottom for the equator, +30° latitude, and +60° latitude for this cylindrical equal-area projection). The craters within the given radius for each bin were then plotted as CSFDs similar to Fig. 3a. If there was a diameter at which the secondary crater CSFD became greater than the primary crater CSFD, that was saved as the value for the bin (top row). If it reached half as much as the primaries, that was the latitude/longitude bin for the middle row, and one-third as much was the value for the bottom row. This transition diameter is color-coded per the legend at the bottom-left, and bins where the primary crater population dominated throughout were left as empty (transparent). These are all overlaid on MOLA shaded relief maps (Smith et al., 2001).

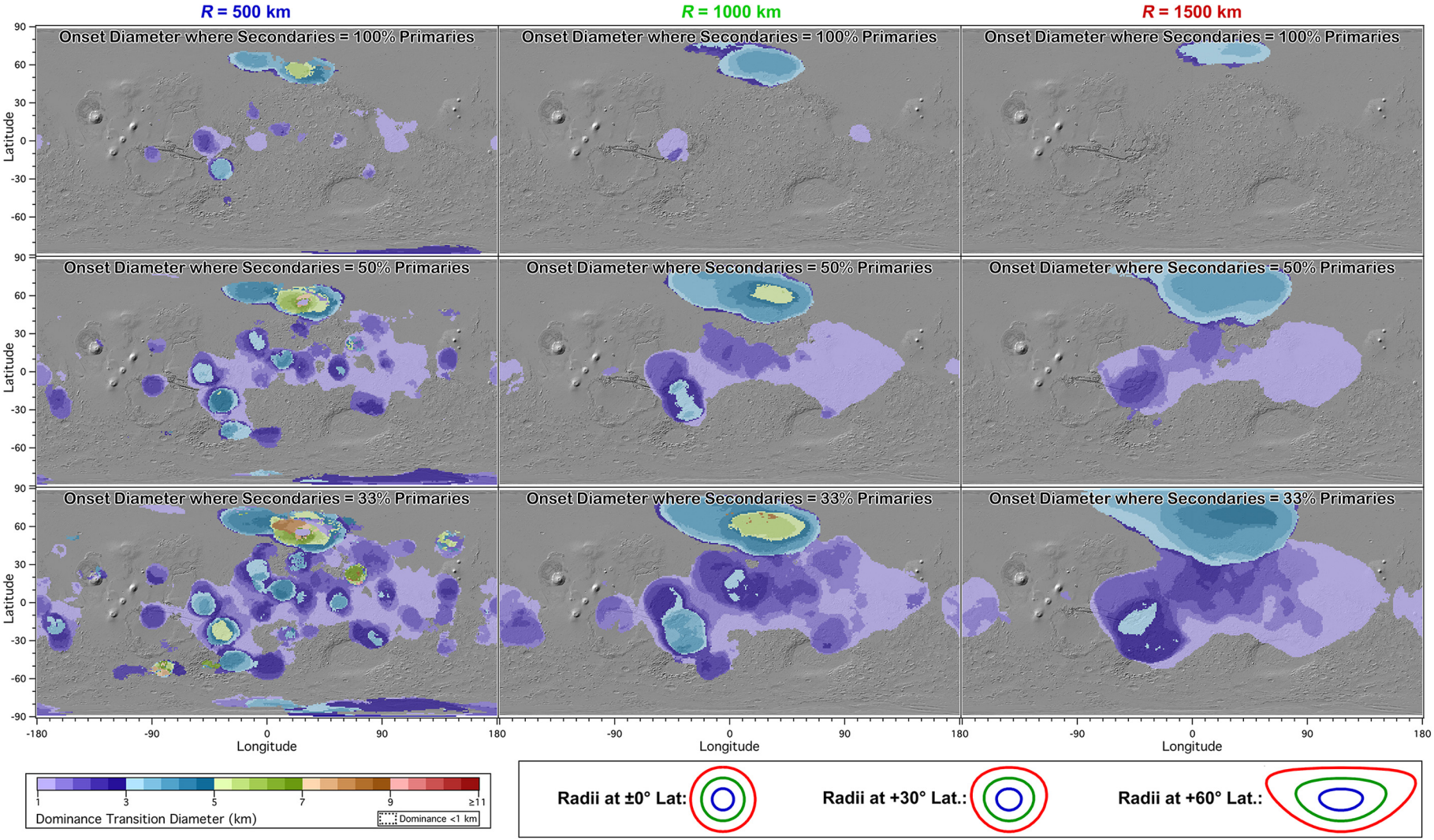

Fig. 5. Same as Fig. 4 except results are from ISFDs, not CSFDs.

cations: Up to $D \approx 6$ km centered on Lyot and $D \approx 4$ km centered on Lomonosov; up to $D \approx 4$ km in the broad area between Holden crater and Ladon basin; up to $D \approx 2$ km in the area between Tharsis, the outflow of Valles Marineris, Cryse, near the south pole, southwest of Syrtis Major, the middle of Arabia Terra, near Oudemans crater, and north of Galle crater; and up to $D \approx 1$–1.5 km over a broad region of Isidis and south of Isidis basin, Elysium basin, and a broad region just west of Terra Meridiani. These trends are reproduced in Fig. 4 except at smaller diameters, indicating that, when combined with the population of larger craters, secondaries are less of a practical issue (this is due to the SFD slope being steeper for secondaries, so they are a smaller fraction of the population at large diameters that is averaged into the CSFDs but not ISFDs). All of these regions are clearly visible in Fig. 2 as hot spots, as well, and many of them were studied individually in Robbins and Hynek (2011b) where the authors mapped these secondary crater fields surrounding individual primary craters to determine both the SFD slopes of the secondaries and their spatial distribution.

The discussion thus-far has focused on what D_t is for secondary craters being equal to or greater than the population of primary craters. Maps were also produced (Figs. 4–5, center and bottom rows) for if one lowers the threshold and instead were to ask, at what diameter do secondary craters equal half the population of primary craters (so are 33% the total population), or at what diameter secondary craters equal one-third the number of primary craters (so are 25% the total population). These can be used in two ways: If one thinks that this study underestimated the number of secondary craters, then lowering the threshold will account for this (provided they were underestimated uniformly across the globe); or, if one has a lower tolerance for secondary craters in their study, then a lower threshold map better describes at what diameter a researcher must remain above before worrying about secondary crater contamination.

When averaged over large, regional scales ($R = 1500$ km), one can see that secondary craters account for 25% of the total crater population for a maximum of $D \gtrsim 2.2$ km, and this is again centered north of Lyot crater; in this broad region, 25% of craters $D \approx 4.6$ km that are produced are secondaries. The other broad, regional area where secondaries dominate at diameters $D \gtrsim 1.4$ km (or, for $D \approx 3$ km) is centered along the large outflow channels of Valles Marineris and Ladon basin. Globally, when wanting to analyze craters $D \geq 1$ km over a large area, these data (Fig. 4, bottom-right) show that one is generally safe over the majority of the planet from secondary crater contamination at the >25% level. However, if one is analyzing small craters only, then the data show (Fig. 5, bottom-right) they would need to be cautious of secondary crater contamination at the >25% level for craters $D \lesssim 3$ km over much of the planet. When shrinking the area to average over $R = 500$ km, and again keeping the threshold at 25% of the total population, numerous hotspots are visible. The additional hotspots at this lower threshold are mainly around Mie crater (50°N, 150°E, $D \approx 100$ km) and surrounding Lowell crater (−50°N, −80°E, $D \approx 200$ km) (these are most apparent in Fig. 5, and the Lowell hot spot is not in Fig. 4). The dominance level reaches diameters as large as $D \approx 7$ km, meaning that in a very few locations, when averaged over a $\sim 800{,}000$ km^2 area (0.5% the surface area of Mars), secondary craters are >25% the population of all craters if using craters $D \lesssim 7$ km. These indicate that when studying many places on the planet, researchers who cannot have more than one-quarter of their crater population be secondary craters must pay careful attention and avoid them even when studying craters at the ∼few-km scale, and especially at smaller diameters.

3.3. Correlation with surface chronostratigraphic epoch

While regional effects can drive different onsets of secondary crater contamination, there is good reason to expect that the onset diameter will be dependent on terrain age: While older terrain has many large craters that can produce ∼km-scale secondaries, younger terrain simply has not had time to accumulate enough large craters to make these $D \sim$ km secondary craters (see Neukum and Ivanov, 1994; McEwen et al., 2005). This is tested with the latest version of the global Mars geologic maps (Tanaka et al., 2014b). The new maps, unlike previous versions (Scott and Tanaka, 1986; Greeley and Guest, 1987), do not have strict unit epochs in all cases, meaning that while there are Late, Middle, and Early Noachian units, there are also areas simply classified as Noachian and others as Hesperian–Noachian or Amazonian–Noachian, and these cover non-trivial areas of the planet. For this analysis, the planet was separated as Tanaka et al. (2014a) do into 14 different units: N, eN, mN, lN, H, HN, eH, lH, A, AN, AH, eA, mA, and lA (e = Early, m = Mid, l = Late, N = Noachian, H = Hesperian, and A = Amazonian).

Then, ISFDs and CSFDs were created for each region to examine D_t. This was then repeated after grouping everything into three "macro" units: N, H, A, where we did not include any that crossed over chronostratigraphic boundaries (HN, AN, and AH, which comprise $2.6 \cdot 10^7$ km^2, or 18% of the planet). From the CSFDs, the percentage of secondary craters that comprised the $D \geq 5$ km and ≥ 1 km populations were measured, and the ≥ 1 km populations were also extrapolated as discussed in Section 3.1 to provide a "corrected" estimate if the size-distribution at larger diameters remained consistent through the $D = 1$ km point. These fits were also used to estimate D_t. The results are shown in Fig. 6.

Theoretically, these would show a simple trend of a decreasing percentage of secondary craters, and a smaller D_t, as one comes closer to the present time because the large primaries needed to form km-scale secondaries have not had time to form. At first glance Fig. 6 does not show this tend. First, the results of the 14 unit types are scattered with no significant trend. However, this lack of trend could easily be interpreted as small numbers problems: Despite the hundreds of thousands of craters in this study, several of the units cover just a few-percent of Mars' surface area and contain a few dozen or hundred craters (*e.g.*, lA has only 75 secondary craters $D \geq 1$ km identified). Therefore, it is the larger, grouped epochs that should be looked to for a trend.

The broader Hesperian versus Amazonian terrains do show what one would expect, where secondaries make up 1.2% of $D \geq 5$ km craters on Hesperian terrain and 0.8% on Amazonian. The corrected population of $D \geq 1$ km craters shows that secondaries are about 37% the population on Hesperian terrain and 17% on Amazonian terrain. Meanwhile, the transition diameter is extrapolated to about 0.75 km ("3/4 km") and 0.5 km ("1/2 km") on the two, respectively. The ancient Noachian terrain does not show a similar trend relative to Hesperian, but that can be explained by erosion: Numerous studies have indicated extensive resurfacing across the globe around the transition from the Noachian to Hesperian epochs, in the amount of ∼1 km of terrain removal, which would destroy craters $D <$ 10–20 km (*e.g.*, Chapman and Jones, 1977; Tanaka et al., 1988; Craddock and Maxwell, 1993; Craddock and Howard, 2002; Forsberg-Taylor et al., 2004; Boyce and Garbeil, 2007; Hoke and Hynek, 2009; Robbins et al., 2013). Others, including Irwin et al. (2013), have shown that craters $D \lesssim 5$ km are unlikely to be older than the Hesperian. This would remove the majority of km-scale secondary craters, leaving the majority of $D > 10$ km primary craters. Therefore, the type of trend actually observed – where secondary craters emplaced on Noachian terrain are similar to those on Hesperian terrain – is what one would expect given this context.

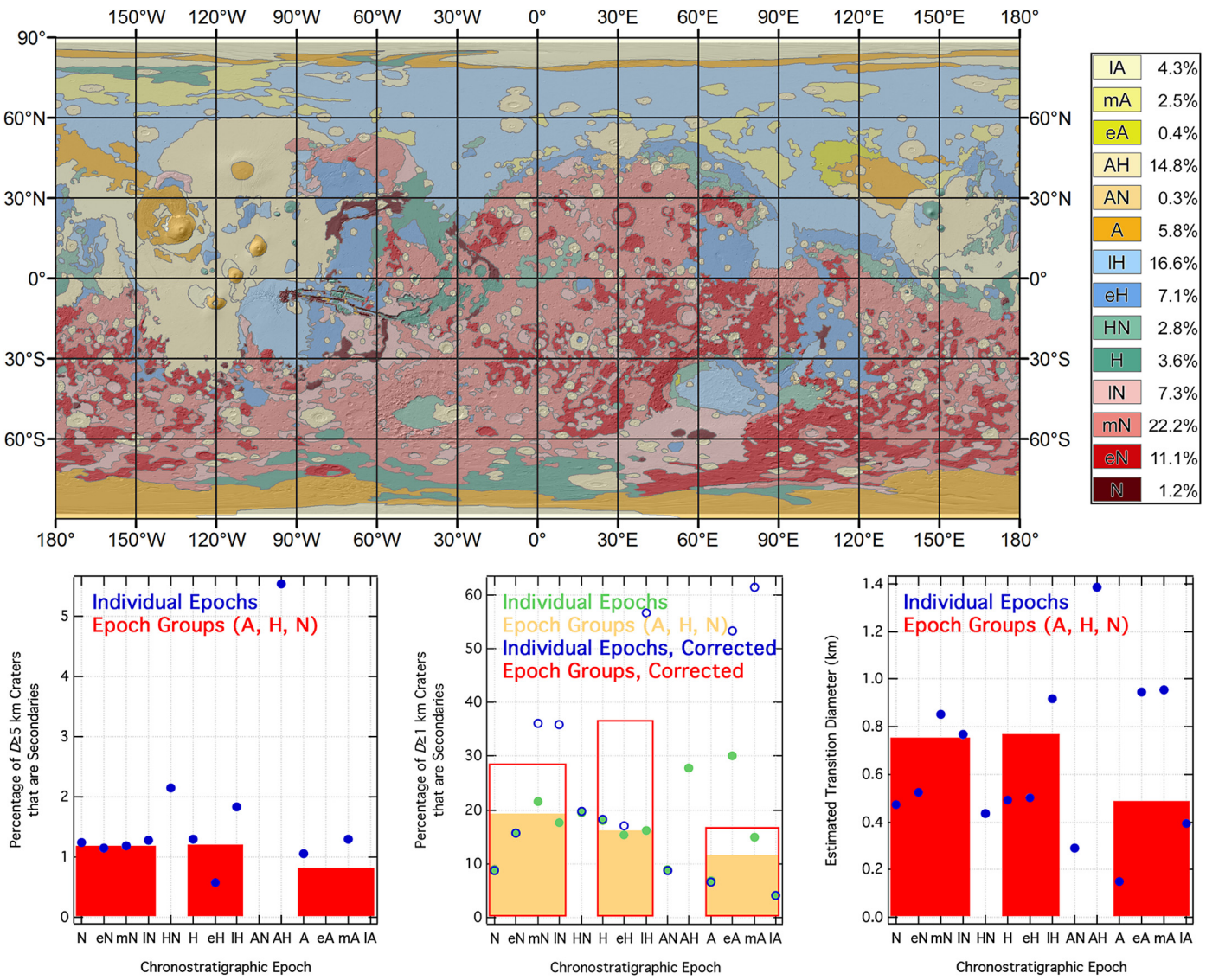

Fig. 6. Top – Martian geologic maps (Tanaka et al., 2014b) showing the 14 chronostratigraphic units which include Noachian (N), Hesperian (H), Amazonian (A) undifferentiated units, units separated into Late (l), Middle (m), and Early (e) divisions, and some that span epoch boundaries; color scheme is per Tanaka et al. (2014a), and percentages next to each unit indicate the fraction of the planet classified as each unit. All Amazonian terrain is 13.0% of the planet, Hesperian is 27.3%, and Noachian is 41.7%. Bottom – the results of examining CSFD and population results of primary and secondary craters once separated into each of the 14 units (circles) or when grouped together into all N, H, and A units (bars). The bottom-left graph shows the percentage of $D \geq 5$ km craters that are secondaries, and the bottom-middle shows the percentage of $D \geq 1$ km craters that are secondaries as measured (green/yellow) and as extrapolated (see text; blue/red). The bottom-right graph shows the extrapolated (or measured – AH only) transition diameter, D_t.

4. Conclusions and discussion

In this work, we have characterized all Martian impact craters $D \geq 1$ km as secondary or primary craters; we have done this in a conservative manner, and we estimate that we may have under-represented the number of secondary craters that currently exist on Mars by as much as a factor of 2 for craters $D \lesssim 2$ km. Even if that is not the case, based only on the craters we identified, secondary craters globally number ≈24% as many as primary craters, meaning they comprise ≈19% the total population of $D \geq 1$ km craters (Fig. 3b); the production of secondaries is ≈26% of all craters $D \approx 1$ km (Fig. 3a). Since we expect to have underestimated the 1–2 km secondary crater population by at least a factor of ∼2, the actual percentage is higher, secondaries comprising ∼33% of the total population if the factor of 2 is correct. This is contrary to predictions and conclusions from the models of various papers, such as Neukum et al. (1975) or Werner et al. (2009), the latter which stated, "the percentage of hypothetically globally unrecognized secondary craters is usually less than 5% for any measurement and has a minor effect on ages … [and we] conclude that crater count measurements are 'contaminated' by secondary cratering by percentages smaller than the assumed statistical error".

We are releasing these maps as well as an update to the Robbins and Hynek (2012) crater database. Besides minor corrections and additional formal names approved by the International Astronomical Union in the past two years, the main change is the additional data column indicating if a crater is likely to be a secondary. If the SECONDARY column is empty, the crater is assumed, by default, to be a primary crater. If instead it has a value entered, it was flagged in this study as a probable primary crater. This database update is available both at http://craters.sjrdesign.net and the United States Geologic Survey's repository at http://webgis.wr.usgs.gov/pigwad/down/mars_crater_consortium.htm.

For most applications of crater populations (*e.g.*, age-modeling, population statistics, dynamical modeling of impactors), the ∼25% contamination level we found is not trivial, and this work indicates that one cannot simply use a crater population blindly and expect an accurate outcome despite the hundreds of published studies that do use these craters. While we do not have the presumption to flatly state that, based on this work, all those previous studies are wrong, it is not as bad as it may seem based on the results presented in Section 3.3: The vast majority of studies that use small, kilometer-scale craters (including some published by these authors), are done on very young, Amazonian-aged terrain, which show less contamination at these diameters than older terrain because there have been no large craters that yet formed since that terrain was last resurfaced that could produce the multitude of kilometer-scale secondaries seen on older terrain. In other words, one should be cognizant of the global contamination (Fig. 3), but the more useful data are the regional contamination maps (Figs. 4–5).

We find that previous work that has limited crater studies to $D > 5$ km due to secondary craters is reasonable, for secondary craters are only ≈1.5% the global population of $D \geq 5$ km craters (and ≈4.7% of the craters $D \approx 5$ km that are produced are secondary craters). We also estimate the transition diameter, globally, where the cumulative number of secondary craters is equal to that of primary craters is $D_t \approx 0.75$ km.

While this is broadly useful, more regional and local results are needed to be useful for individual studies of certain regions of the planet. For example, if one were creating global geologic maps and wanted to extract craters from a global crater database to estimate relative stratigraphy and model ages (*e.g.*, Tanaka et al., 2014a), then we would recommend using Fig. 4's bottom-right plot. It shows that, as a general rule, almost all terrains can be classified as being dominated by primary craters so long as one relies on $D > 2$ km craters; the one exception is near Lyot crater, but the northern plains are generally mapped as one, broad, Hesperian lowland unit (Tanaka et al., 2014b) and so would tend to average out. We can also say after an examination of our maps with the latest geologic maps (Figs. 4–6) that it does not appear as though secondary craters affected unit epoch attribution in the most recent geologic maps (Tanaka et al., 2014b). At the opposite extreme, if one were performing detailed mapping of the Ladon basin, Fig. 5's bottom-left plot would be best used, and it suggests the researcher must be extremely careful of secondary craters unless restricting themselves to $D > 6$ km. Otherwise, detailed age differences among the units could easily be attributable to slightly closer or farther proximity to/from a large primary that has produced numerous secondaries. The ISFD version should be used instead of the CSFD because mapping smaller units often means one is limited to smaller craters, and the ISFD is also a more conservative estimate. Based on the stronger regional rather than age trends (contrast Figs. 4 and 5 with Fig. 6), we recommend using these over using a generalized value for a terrain age.

While this work has focused on Mars, and it is the first of its kind to be conducted for any body, the implications (if not applications) to other planets and bodies directly follow because they are the same: Not only are primary crater populations required for estimating the ages – both absolute and relative – but primary crater populations are needed without secondary contamination to estimate the population of impactors (related to impact hazards) and to understand dynamical processes, such as ejecta exchange within gas giant moon systems and potential apex/antapex cratering asymmetries on tidally locked satellites such as Earth's moon. Only by having a global census of impact craters and classifying them as primary or secondary can we gain a better understanding of how they affect global, regional, and local crater populations and use those to better understand the processes that create those populations to begin with.

Acknowledgements

The authors thank A. McEwen and one anonymous reviewer for their efforts. We also thank C. Fortezzo for supplying the latest iteration of the Mars global geologic maps. Support for the authors was made possible through NASA Award NNX10AL65G.

References

Barlow, N.G., 1988. Crater size-frequency distributions and a revised Martian relative chronology. Icarus 75, 285–305. http://dx.doi.org/10.1016/0019-1035(88)90006-1.

Bierhaus, E.B., Chapman, C.R., Merline, W.J., 2005. Secondary craters on Europa and implications for cratered surfaces. Nature 437, 1125–1127. http://dx.doi.org/10.1038/nature04069.

Bottke, W.F., Nesvorny, D., Durda, D.D., 2005. Are most small craters primaries or secondaries: insights from asteroid collisional/dynamical evolution models. Lunar Planet. Sci. Conf. 36. Abstract #1489.

Boyce, J.M., Garbeil, H., 2007. Geometric relationships of pristine Martian complex impact craters, and their implications to Mars geologic history. Geophys. Res. Lett. 34, L16201. http://dx.doi.org/10.1029/2007GL029731.

Chapman, C.R., Haefner, R.R., 1967. A critique of methods for analysis of the diameter-frequency relation for craters with special application to the Moon. J. Geophys. Res. 72, 549–557. http://dx.doi.org/10.1029/JZ072i002p00549.

Chapman, C.R., Jones, K.L., 1977. Cratering and obliteration history of Mars. Annu. Rev. Earth Planet. Sci. 5, 515–540. http://dx.doi.org/10.1146/annurev.ea.05.050177.002503.

Craddock, R.A., Howard, A.D., 2002. The case for rainfall on a warm, wet early Mars. J. Geophys. Res. 107 (E11), 5111. http://dx.doi.org/10.1029/2001JE001505.

Craddock, R.A., Maxwell, T.A., 1993. Geomorphic evolution of the Martian highlands through ancient fluvial processes. J. Geophys. Res. 98 (E2), 3453–3468. http://dx.doi.org/10.1029/92JE02508.

Crater Analysis Techniques Working Group, 1979. Standard techniques for presentation and analysis of crater size-frequency data. Icarus 37, 467–474. http://dx.doi.org/10.1016/0019-1035(79)90009-5.

Edwards, C.S., Nowicki, K.J., Christensen, P.R., Hill, J., Gorelick, N., Murray, K., 2011. Mosaicking of global planetary image datasets: 1. Techniques and data processing for Thermal Emission Imaging System (THEMIS) multi-spectral data. J. Geophys. Res. 116, E10008. http://dx.doi.org/10.1029/2010JE003755.

Fassett, C.I., Head, J.W., 2011. Sequence and timing of conditions on early Mars. Icarus 211, 1204–1214. http://dx.doi.org/10.1016/j.icarus.2010.11.014.

Forsberg-Taylor, N.K., Howard, A.D., Craddock, R.A., 2004. Crater degradation in the Martian highlands: morphometric analysis of the Sinus Sabaeus region and simulation modeling suggest fluvial processes. J. Geophys. Res. 109, E05002. http://dx.doi.org/10.1029/2004JE002242.

Greeley, R., Guest, J.E., 1987. Geologic map of the eastern equatorial region of Mars. USGS Misc. Inv. Series Map I-1802-B.

Guinness, E.A., Arvidson, R.E., 1977. On the consistency of the lunar cratering flux over the past 3.3×10^9 yr. Lunar Planet. Sci. Conf. Proc. 8, 3475–3494.

Hartmann, W.K., 2005. Martian cratering 8: isochron refinement and the chronology of Mars. Icarus 174, 294–320. http://dx.doi.org/10.1016/j.icarus.2004.11.023.

Hoke, M.R.T., Hynek, B.M., 2009. Roaming zones of precipitation on ancient Mars as recorded in valley networks. J. Geophys. Res. 113, E8. http://dx.doi.org/10.1029/2008JE003247.

Irwin, R.P., Tanaka, K.L., Robbins, S.J., 2013. Distribution of Early, Middle, and Late Noachian cratered surfaces in the Martian highlands: implications for resurfacing events and processes. J. Geophys. Res. 118, 278–291. http://dx.doi.org/10.1002/jgre.20053.

Ivanov, B.A., 2001. Moon/Mars cratering rate ratio estimates. Chronol. Evol. Mars 96, 87–104.

McEwen, A.S., Bierhaus, E.B., 2006. The importance of secondary cratering to age constraints on planetary surfaces. Annu. Rev. Earth Planet. Sci. 34, 535–567. http://dx.doi.org/10.1146/annurev.earth.34.031405.125018.

McEwen, A.S., Preblich, B.S., Turtle, E.P., Artemieva, N.A., Golombek, M.P., Hurst, M., Kirk, R.L., Burr, D.M., Christensen, P.R., 2005. The rayed crater Zunil and interpretations of small impact craters on Mars. Icarus 176, 351–381. http://dx.doi.org/10.1016/j.icarus.2005.02.009.

Neukum, G., 1983. Meteoritenbombardement and Datierung planetarer Oberflächen. Habilitation dissertation for faculty membership. Univ. of Munich. 186 pp.

Neukum, G., Ivanov, B.A., 1994. Crater size distributions and impact probabilities on Earth from lunar, terrestrial-planet, and asteroid cratering data. In: Gehrels, T., Matthews, M.S., Schumann, A.M. (Eds.), Hazards Due to Comets and Asteroids. Univ. of A. Press, ISBN 978-0816515059. 359 pp.

Neukum, G., König, B., Arkani-Hamed, J., 1975. A study of lunar impact crater size-distributions. Moon 12, 201–229. http://dx.doi.org/10.1007/BF00577878.

Neukum, G., Ivanov, B.A., Hartmann, W.K., 2001. Cratering records in the inner solar system in relation to the lunar reference system. Chronol. Evol. Mars 96, 55–86.
Oberbeck, V.R., Morrison, R.H., 1974. Laboratory simulation of the herringbone pattern associated with lunar secondary crater chains. Moon 9, 415–455. http://dx.doi.org/10.1007/BF00562581.
Popova, O., Hartmann, W.K., Nemtchinov, I.V., Richardson, D.C., Berman, D.C., 2007. Crater clusters on Mars: shedding light on Martian ejecta launch conditions. Icarus 190, 50–73. http://dx.doi.org/10.1016/j.icarus.2007.02.022.
Preblich, B.S., McEwen, A.S., Studer, D.M., 2007. Mapping rays and secondary craters from the Martian crater Zunil. J. Geophys. Res. 112, E05006. http://dx.doi.org/10.1029/2006JE002817.
Robbins, S.J., 2013. Revised lunar cratering chronology for planetary geological histories. Lunar Planet. Sci. Conf. 44. Abstract #1619.
Robbins, S.J., submitted for publication. New crater calibrations for the lunar crater-age chronology. Earth Planet. Sci. Lett.
Robbins, S.J., et al., 2014. The variability of crater identification among expert and community crater analysts. Icarus 234, 109–131. http://dx.doi.org/10.1016/j.icarus.2014.02.022.
Robbins, S.J., Hynek, B.M., 2011a. Distant secondary craters from Lyot Crater, Mars, and implications for ages of planetary bodies. Geophys. Res. Lett. 38, L05201. http://dx.doi.org/10.1029/2010GL046450.
Robbins, S.J., Hynek, B.M., 2011b. Secondary crater fields from 24 large primary craters on Mars: insights into nearby secondary crater production. J. Geophys. Res. 116, E10003. http://dx.doi.org/10.1029/2011JE003820.
Robbins, S.J., Hynek, B.M., 2012. A new global database of Mars impact craters $\geq$1 km: 1. Database creation, properties, and parameters. J. Geophys. Res. 117, E05004. http://dx.doi.org/10.1029/2011JE003966.
Robbins, S.J., Hynek, B.M., Lillis, R.J., Bottke, W., 2013. The large crater impact history of Mars: the effect of different model crater age techniques. Icarus 225, 173–184. http://dx.doi.org/10.1016/j.icarus.2013.03.019.
Scott, D.H., Tanaka, K.L., 1986. Geologic map of the western equatorial region of Mars. USGS Mic. Inv. Ser. Map I-1802-A.
Shoemaker, E.M., 1962. Interpretation of lunar craters. In: Kopal, Z. (Ed.), Physics and Astronomy of the Moon. Academic Press, New York, pp. 283–359.
Shoemaker, E.M., 1965. Preliminary analysis of the fine structure of the lunar surface in Mare Cognitum. In: Heiss, W.N., Menzel, D.R., O'Keefe, J.A. (Eds.), The Nature of the Lunar Surface. Johns Hopkins Univ. Press, Baltimore, MD, pp. 23–77.
Shoemaker, E.M., Hait, M.H., Swann, G.A., Schleicher, D.L., Dahlem, D.H., Schaber, G.G., Sutton, R.L., 1970. Lunar regolith at tranquility base. Science 167 (3918), 452–455. http://dx.doi.org/10.1126/science.167.3918.452.
Shoemaker, E.M., Robinson, M.S., Eliason, E.M., 1994. The South Pole Region of the Moon as Seen by Clementine. Science 266, 1851–1854. http://dx.doi.org/10.1126/science.266.5192.1851.
Smith, D.E., et al., 2001. Mars Orbiter Laser Altimeter: experiment summary after the first year of global mapping on Mars. J. Geophys. Res. 106, 23689–23722. http://dx.doi.org/10.1029/2000JE001364.
Strom, R.G., Croft, S., Barlow, N.G., 1992. The Martian impact cratering record. In: Kieffer, H., Jakosky, B., Snyder, C.W., Matthews, M.S. (Eds.), Mars. Univ. Ariz. Press, Tucson, pp. 383–423.
Tanaka, K.L., 1986. The stratigraphy of Mars. J. Geophys. Res. 91, E139–E158. http://dx.doi.org/10.1029/JB091iB13p0E139.
Tanaka, K.L., Isabel, N.K., Scott, D.H., Greeley, R., Guest, J.E., 1988. The resurfacing history of Mars: a synthesis of digitized, viking-based geology. Lunar Planet. Sci. Conf. Proc. 18, 665–678.
Tanaka, K.L., Robbins, S.J., Fortezzo, C.M., Skinner Jr., J.A., Hare, T.M., 2014a. The digital global geologic map of Mars: unit chronostratigraphic ages, topographic characteristics, and updated resurfacing history. Planet. Space Sci. 95, 11–26. http://dx.doi.org/10.1016/j.pss.2013.03.006.
Tanaka, K.L., Skinner Jr., J.A., Dohm, J.M., Irwin III, E.J., Kolb, E.J., Fortezzo, C.M., Platz, T., Michael, G.G., Hare, T.M., 2014b. Geologic map of Mars: U.S. Geological Survey Scientific Investigations Map 3292, pamphlet 43 p., 1 sheet, scale 1:20,000,000. http://dx.doi.org/10.3133/sim3292.
Werner, S.C., 2008. The early Martian evolution: constraints from basin formation ages. Icarus 195, 45–60. http://dx.doi.org/10.1016/j.icarus.2007.12.008.
Werner, S.C., Ivanov, B.A., Neukum, G., 2009. Theoretical analysis of secondary cratering on Mars and an image-based study on the Cerberus Plains. Icarus 200, 406–417. http://dx.doi.org/10.1016/j.icarus.2008.10.011.